# Fine Micro-welding of Thin Stainless Steel Sheet by High Speed Laser Scanning

Yasuhiro OKAMOTO[*], Arnold GILLNER[**], Alexander OLOWINSKY[**], Jens GEDICKE[**] and Yoshiyuki UNO[*]

[*] *Nontraditional Machining Laboratory, Graduate School of Natural Science and Technology, Okayama University, 3-1-1 Tsushimanaka, Okayama 700-8530, Japan*
*E-mail: okamoto@mech.okayama-u.ac.jp*
[**] *Fraunhofer Institute for Laser Technology ILT, Steinbachstrasse 15, 52074 Aachen, Germany*

Fraunhofer Institute for Laser Technology had developed the SHADOW® welding technique, in which high speed joining with minimal distortion is possible using a pulsed Nd:YAG laser. The possibility of high speed, high quality welding had been also reported by use of a single-mode fiber laser. The combination of micro-beam and high speed laser scanning offers potential advantages for thin metal sheet welding. Therefore, the characteristics of micro-welding for thin stainless sheet were investigated here by high speed laser scanning with both single-mode fiber laser and pulsed Nd:YAG laser. The results were a narrow welding region obtained using a laser beam with a large focus diameter of 160 μm without pulse control, while a small focus diameter of 22 μm was found in general to provide good control of the welding state. A small focus diameter can result in an excellent welding seam from the start, even without pulse control. The penetration depth could be controlled by the energy density with a small focus diameter. For the smaller beam foucus diameter, an unique periodic structure appeared at high beam scanning velocities. Moreover, by using a laser beam with a small focus diameter, the overlap welding of 25 μm thickness sheet could be successfully performed, regardless of the presence of a small gap distance between two sheets.

DOI: 10.2961/jlmn.2008.02.0007

**Keywords:** SHADOW®, thin sheet, SM fiber laser, Nd:YAG laser, high speed scanning, micro spot

## 1. Introduction

In recent years, since the size of product becomes smaller in electrical and electronics industries, then the joining of thin metal sheet has been required. The flexibility of process is important according to the accessibility in the case of small component. Fraunhofer Institute for Laser Technology ILT had developed the SHADOW® welding technique [1-4], in which high speed joining with minimal distortion is possible using a pulsed Nd:YAG laser by a non-contact process. The processing time is defined by the pulse duration of pulsed laser, and the processing length was determined by the combination of pulse duration and velocity of laser beam. Besides, the welded joints show a smooth surface compared to the spaced spot welding.

Prof. Miyamoto et al. at Osaka University had reported the possibility of high speed and high quality welding by use of a single- mode fiber laser [5]. However, the distortion is easy to occur by the small heat input in the case of thin sheet. Accordingly, the welding with low heat input is necessary to avoid the large distortion. A smaller beam spot from the single-mode fiber laser and the thin-disk laser can increase the intensity, which leads to the low energy input into the workpiece with high speed beam scanning. It is expected that the combination of micro-beam and high speed laser scanning offers potential advantages for thin metal sheet welding. Moreover, the welding seam length can be relieved from the restrictions of pulse duration in SHADOW® technique by using the cw fiber laser and the thin-disk laser. Therefore, the characteristics of micro-welding for thin metal sheet were investigated by high speed laser scanning, in which the welding was carried out by the scanner system with both single-mode cw fiber laser and pulsed Nd:YAG laser.

## 2. Experimental procedures

Figure 1 shows schematic diagram of experimental setup. Single-mode cw Yb-fiber laser (SPI SP-100C) of 1090 nm in wavelength and pulsed Nd:YAG laser (HAAS HL62P) of 1064 nm in wavelength were used as a laser source in this study. The laser beam of 5.45 mm in diameter from the fiber laser was expanded by 2 times beam expander. The laser beam of pulsed Nd:YAG laser was collimated to 18 mm with 100 mm focal length lens from the fiber of 200 μm in diameter. Both lasers were delivered by optical fiber, and these laser beams were focused by a telecentric type fθ lens of 80 mm in focal length. When the laser source was changed, optical fiber and collimation lens

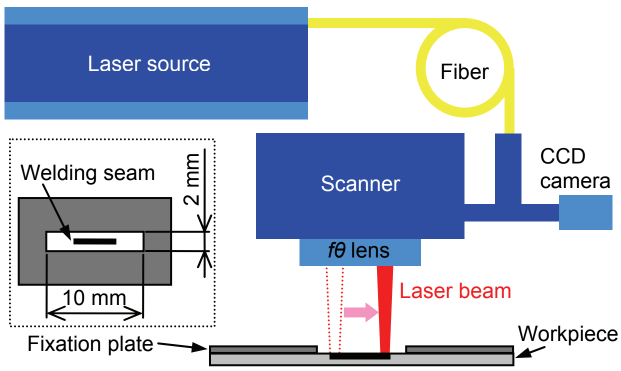


**Fig. 1** Schematic diagram of experimental setup and fixation method of workpiece.

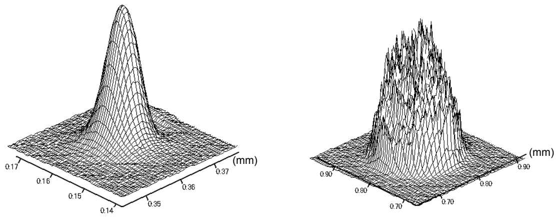


(a) Single-mode cw fiber laser (b) Pulsed Nd:YAG laser

**Fig. 2** Intensity distribution of laser beam at focusing point.

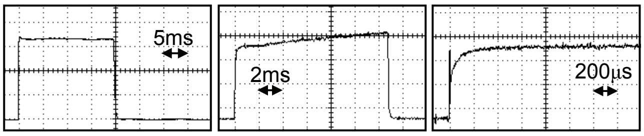


(a) Pulsed laser (P = 30 W) (b) SM fiber laser (P = 15 W) (c) Initial spike of SM fiber laser (P = 15 W)

**Fig. 3** Pulse waveforms.

were replaced at the scanner head. The stainless steel (X5CrNi18 10) of 25 μm was used as a workpiece, which was set on the mounting device. The workpiece was fixed by the fixation plate with a hole of dimension 2 by 10 mm. The welding experiment was carried out at focusing point in the atmosphere without a shielding gas. The position of laser beam was controlled by the scanner system (SCANLAB working field 40 by 40 mm). The welding length of single-mode fiber laser was set at 6 mm, while the welding length of pulsed Nd:YAG laser was determined by the multiplication of a constant pulse duration 20 ms and velocity.

Figure 2 shows the intensity distribution of both lasers measured by the micro spot monitor (PRIMES). The single-mode cw Yb-fiber laser is excellent beam mode of $TEM_{00}$ and its spot diameter was 22 μm at the focusing point. On the other hand, the pulsed Nd:YAG laser has the multi-mode, and its spot diameter was 160 μm at the focusing point. The spot diameter of both lasers was almost equal under every laser power condition.

Figure 3 shows the waveform of pulsed Nd:YAG laser and single-mode fiber laser measured by high-speed photo detector. As shown in Fig. 3 (a), pulse waveform of pulsed Nd:YAG laser could be controlled to a rectangular shape. On the other hand, the single-mode fiber laser was controlled by setting the current of pumping diode laser, and the laser power gradually increased with time as shown in Fig. 3 (b). The laser power at the end point of pulse was defined as the laser power of single-mode fiber laser. Besides, the fiber laser had the spike at the initial region as shown in Fig. 3 (c). It was reported that the drilling for metal sheet could be carried out by the initial spike, which is ten times higher than the set value of laser power [6]. However, since its value was almost equal to the set laser power under this experimental condition, it is considered that this initial spike would have little influence on the welding results compared to the former report.

## 3. Bead on plate weld

### 3.1 Welding region for thin sheet

Since the thickness of workpiece is very thin with 25 μm, the heat flux is reflecting at the backside of workpiece.

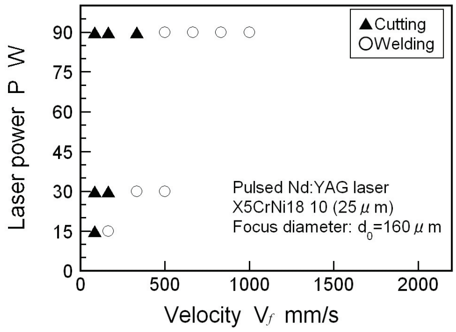


(a) Pulsed Nd:YAG laser

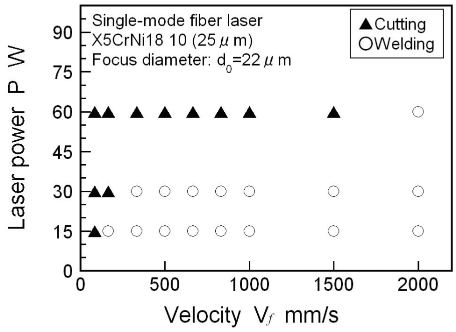


(b) Single-mode fiber laser

**Fig. 4** Map of welding or cutting as functions of velocity of laser beam and laser power.

Accordingly, the temperature of thin workpiece becomes higher due to a heat accumulation compared to thicker workpiece [3]. Therefore, accurate control of laser power and velocity of beam scanning is required. First, the welding region is investigated under several irradiation conditions by changing the laser power and the velocity of beam scanning as shown in Fig. 4. In the case of pulsed Nd:YAG laser, the slow velocity of beam scanning became the cutting condition under every selected laser power. Increasing the beam scanning velocity, the welding region appeared, and its region became wider with increasing the laser power. After the welding region, the workpiece could not be melted any longer. On the other hand, the single-mode fiber laser with a small focus diameter of 22 μm can melt the workpiece of 25 μm in thickness sufficiently by less than 30 W up to 2000 mm/s in the velocity of beam scanning, and its controllable region of welding is wider than the pulsed Nd:YAG laser with a larger focus diameter of 160 μm. The single-mode fiber laser can perform the welding of 25 μm in thickness under the low laser power and the high beam scanning velocity conditions. The combination of low laser power and high beam scanning velocity makes it possible to realize the low energy input per unit length, which leads to the avoidance of distortion.

Figure 5 shows the Scanning Electron Microscope (SEM) photographs of welding seam by the pulsed Nd:YAG laser with a larger focus diameter of 160 μm. Since absorptivity of stainless steel (X5CrNi18 10) is approximately 30 % at 1064 nm, the melted state could not be clearly observed at the start point. In order to avoid this problem of unstable process, the pulse shape modification is effective, in which the pulse has a high peak at the beginning [4]. However, since the diameter of laser beam is larger than 5 times of workpiece thickness, the same

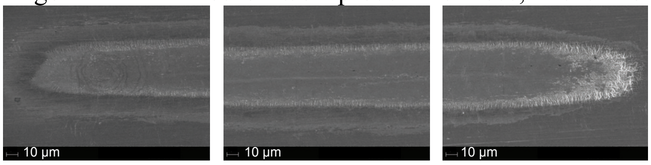


(a) Start (b) Middle (c) End

**Fig. 5** SEM photographs of welding seam by pulsed Nd:YAG laser (P = 30 W, $V_f$ = 333 mm/s, $d_o$ =160 μm).

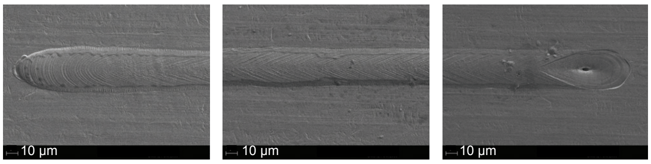


(a) Start (b) Middle (c) End

**Fig. 6** SEM photographs of welding seam by single-mode fiber laser (P = 15 W, $V_f$ = 666 mm/s, $d_o$ =22 μm).

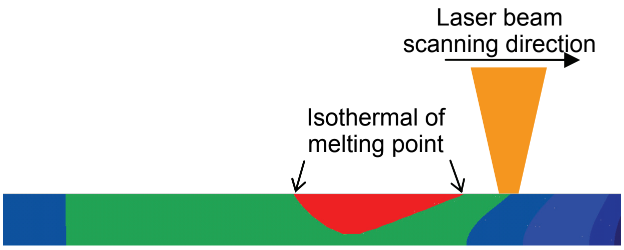


(a) P = 30 W, $V_f$ = 333 mm/s, $d_o$ =160 μm

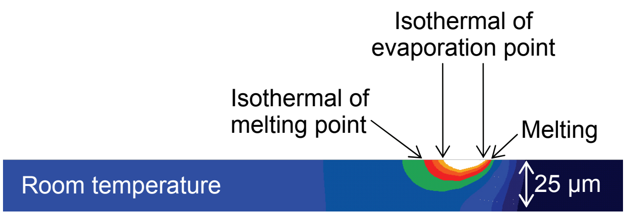


(b) P = 15 W, $V_f$ = 666 mm/s, $d_o$ =22 μm

**Fig. 7** Approximation of temperature in 25 μm thickness sheet.

method with a high peak at the beginning of pulse accompanies the risk to make a hole at the start point. The unavoidable acceleration time of beam scanning makes it difficult to control the input energy into the workpiece at the start of process.

On the other hand, the single-mode fiber laser, used without pulse control, produces good welding from the start of the weld as shown in Fig. 6. The laser beam was effectively absorbed from the start of beam scan, while at the end point a cavity can be observed, which was generated on closing of keyhole as the beam was switched off. In Fig. 6 (a), the widening of top bead width was observed. This widening phenomenon was observed only under low velocity condition. Therefore, it is considered that due to a higher energy input to the surface region of the weld bead, the keyhole extruded the molten material to backward side of laser beam.

Figure 7 shows approximated results of the temperature distribution at the cross section of laser beam scanning line with the steady thermal calculation program 'Laser Weld3D', which was developed by Fraunhofer Institute for Laser Technology. The surface temperature of workpiece was less than the evaporation point under the condition (P

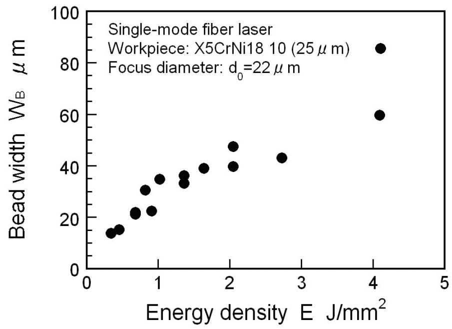


(a) Bead width

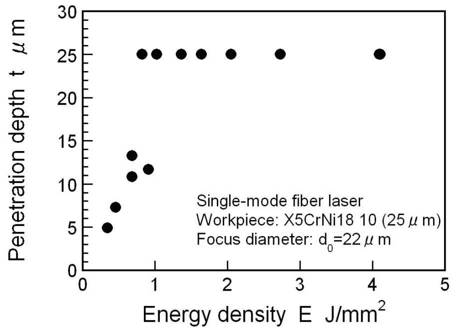


(b) Penetration depth

**Fig. 8** Bead width and penetration depth with energy density by single-mode fiber laser.

= 30 W, $V_f$ = 333 mm/s, $d_o$ =160 μm), that is the heat conduction welding. Therefore, the cavity was not observed at the end point as shown in Fig. 5 (c). The boundary between the welding seam and the base material was not clear. On the other hand, the single-mode fiber laser with a small focus diameter can increase the surface temperature above the evaporation point under the condition (P = 15 W, $V_f$ = 666 mm/s, $d_o$ =22 μm). Also, a part of melted material is moved toward the surface direction as shown in Fig. 6, and the welding seam can be clearly observed with sharp boundary line. From these results, the welding with single-mode fiber laser was mainly investigated, because the small focus diameter is effective to control the welding condition for thin sheet.

### 3.2 Bead width and penetration depth by single-single mode fiber laser

Figure 8 shows the bead width and the penetration depth with the energy density by single-mode fiber laser. The energy density was calculated as shown in equation (1).

$$E = \frac{P}{V_f \times d_0} \qquad (1)$$

where *E* = Energy density, *P* = laser power, $V_f$ = beam scanning velocity, $d_0$ = beam diameter at focus point.

As shown in Fig. 8 (a), the bead width increased proportionately with the energy density less than 1 J/mm$^2$, and increasing rate of bead width became lower at the energy densities higher than 1 J/mm$^2$. The full penetration was accomplished at the energy densities higher than 1 J/mm$^2$, while the quasi penetration welding can be performed at the energy densities less than 1 J/mm$^2$. Also, the penetration depth can be controlled by the energy density with a small focus diameter as shown in Fig. 8 (b). At the energy

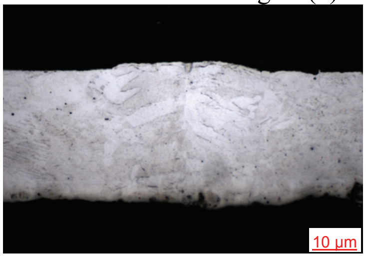


(a) $V_f$ = 666 mm/s

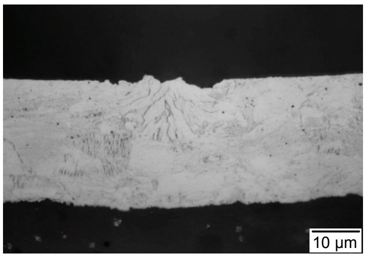


(b) Vf = 1000 mm/s

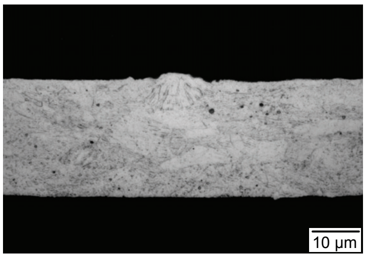


(c) $V_f$ = 2000 mm/s

**Fig. 9** Cross section of 25 μm stainless sheet weld by single-mode fiber laser at laser power 15W.

density 1 J/mm$^2$, the penetration depth increases drastically from 13 μm in penetration depth to 25 μm of full penetration depth.

Figure 9 show the cross section of 25 μm stainless sheet weld by the single-mode fiber laser at laser power 15 W. The fine weld bead was obtained without humping. These shapes of weld bead at high velocity indicate that these welding were carried out by the heat conduction. However, approximated surface temperature was above the evaporation temperature under every condition of single-mode fiber laser with 3.9 × 10$^6$ W/cm$^2$, which is around the boundary region between heat conduction and deep penetration welding with keyhole [2]. Since the surface temperature would be more than evaporation point, the keyhole might be generated. However, the beam scanning velocity was extremely fast, and the depth of keyhole could not become sufficient large size. Then, it is considered that the bead shape is similar to the heat conduction welding. It would be discussed whether this weld bead can be done by heat conduction or by keyhole welding in the further study.

### 3.3 Welding seam structure

Figure 10 shows the welding seam under various scanning velocity conditions. At the velocity of 500 mm/s, the gap between the melted material and the base material can be observed, and the shape of gap is not straight line. The deformation due to the high temperature gradient might be noticed in the case of thin sheet. The workpiece was deformed at the front of laser beam, which was observed by high speed camera imaging. Besides, since the volume

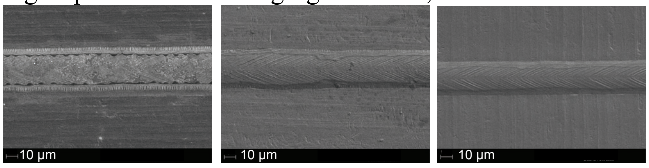


(a) $V_f$ = 500 mm/s (b) $V_f$ = 666 mm/s (c) $V_f$ = 833 mm/s

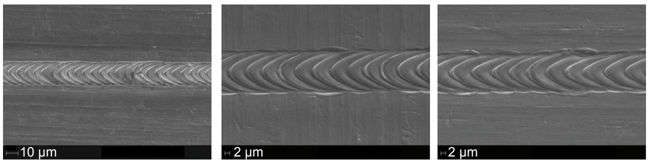


(d) $V_f$ = 1000 mm/s (e) $V_f$ = 1500 mm/s (f) $V_f$ = 2000 mm/s

**Fig. 10** SEM photographs of welding seam for various scanning velocities by single-mode fiber laser at laser power 15 W.

**Table 1** Traveling period between peaks of periodic structure by the average of ten measurements.

| Velocity (mm/s) | 1000 | 1500 | 2000 |
|---|---|---|---|
| Traveling period (μs) | 4.49 | 3.79 | 3.31 |

changes from the liquid phase to the solid phase, the gap might be caused by both the deformation and the volume change. At the velocity of 666 mm/s and 833 mm/s, the excellent fine welding without humping can be performed with bead width less than 30 μm. On the other hand, a periodic structure appeared at the velocities more than 1000 mm/s, in which quasi penetration welding was accomplished. The fluctuation of laser power and intensity distribution is considered as the possibility of the reason for this phenomenon. However, the fluctuation of laser power is not large as shown in Fig. 3. Also, the stability of intensity distribution could be confirmed by the measurement with micro spot monitor, even if the guide fiber was moved. The digitized movement of scanner mirror might be the cause of this periodic structure. Therefore, the traveling period between peaks was calculated in Table 1. The traveling time was not equal under every velocity condition. The minimal position update period of this scanner system is 10 μs, which is longer than the calculated value of traveling period between peaks as shown in Table 1. Therefore, this periodic structure might be caused by material behavior, although there remains a little suspicion that the digitized movement or the fluctuation of laser power and intensity distribution might affect.

## 4. Overlap welding

The overlap welding of two thin sheets (25 μm) was carried out by the single mode fiber laser. As shown in Fig. 11, the fine bead was also obtained without any humping, undercut and drop out. Overlap welding could be successfully performed as shown in Fig. 11 (b), although the small gap remained between two sheets. In the case of thin sheet, even if two sheets could be mounted without gap, a little distortion was unavoidable from the start of laser irradiation. Because the thin sheet is very low rigidity, and the large temperature gradient (see Fig. 7(b)) generates the high thermal stress, which can deform the thin sheet sufficiently. This phenomenon has greatly influence on a line welding compared to a spot welding. If the welding can be performed regardless of small gap distance between two sheets, it is really effective to thin sheet welding technique.

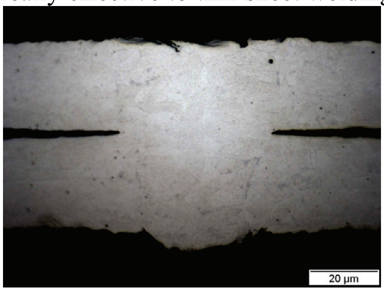


(a) P = 15 W, $V_f$ = 166 mm/s

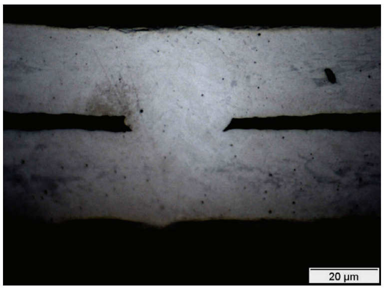


(b) P = 30 W, $V_f$ = 833 mm/s

**Fig. 11** Cross section of two thin sheets welding by single-mode fiber laser with 22 µm focus diameter.

Moreover, low energy input into the workpiece is effective to avoid a large distortion. Therefore, it is considered that the combination of micro beam and high speed laser scanning has many advantages for thin metal sheet welding.

## 5. Conclusions

The characteristics of micro-welding for thin stainless sheet were investigated by high speed laser scanning with both single-mode fiber laser and pulsed Nd:YAG laser. Main conclusions obtained in this study are as follows:

(1) The results were a narrow welding region obtained using a laser beam with a large focus diameter of 160 µm without pulse control, while a small focus diameter of 22 µm was found in general to provide good control of the welding state.

(2) A small focus diameter could result in an excellent welding seam from the start, even without pulse control.

(3) The penetration depth could be controlled by the energy density with a small focus diameter of 22 µm at the energy densities less than 1 J/mm$^2$.

(4) For the small focus diameter, a unique periodic structure appeared at high beam scanning velocities.

(5) The overlap welding of 25 µm thickness could be successfully performed, regardless of the presence of a small gap distance between two sheets by the laser beam with a small focus diameter of 22 µm.

**Acknowledgments**

The authors would like to thank Prof. Dr. R. Poprawe, Fraunhofer Institute for Laser Technology ILT, and Prof. Dr. I. Miyamoto, Osaka University, for their helpful advice and timely guidance throughout this study. The authors are also grateful to Prof. Dr. W. Schulz, Dr. K. Klages and Dipl.-Ing. F. Schmitt, Fraunhofer Institute for Laser Technology ILT, for the informative discussions.

**References**

[1] T. Kramer, A. Olowinsky and F. Durand: SHADOW – A New Welding Technique, Proceedings of SPIE 4637, (2002) p.545.

[2] T. Kramer and A. Olowinsky: Out of SHADOW: Watch Parts in the Spotlight, Proceedings of SPIE Vol. 4977, (2003) p.481.

[3] K. Klages, A. Olowinsky and J. Gedicke: Performance of SHADOW, Proceedings of Laser Assisted Net Shape Engineering in Erlangen, (2004) p.633.

[4] J. Gedicke, A. Olowinsky and K. Klages: Advancements of SHADOW® –Laser beam welding of compression molded copper, Proceedings of LPM2005 in Williamsburg, (2005) On-line.

[5] I. Miyamoto, S. Park and T. Ooie: Ultrafine-Keyhole Welding Process Using Single-Mode Fiber Laser, Proceedings of ICALEO2003 in Jacksonville, (2003) CD-ROM.

[6] W. Harp and J. Tu: Investigation of the Transition from Micro-Drilling to Micro-Welding Using a 300W Fiber Laser, Proceedings of ICALEO2006 in Scottsdale, (2006) CD-ROM.

(Received: April 24, 2007, Accepted: February 21, 2008)